The 6th IBPSA Canada Conference
La 6e conférence d'IBPSA – Canada
Winnipeg, May 19 – 20

CALIBRATION OF MODELED AND MEASURED RESULTS FOR A SINGLE-FAMILY RESIDENTIAL SOLAR SEASONAL STORAGE SYSTEM

David E. BRADLEY[1], Edward J. WHITAKER[2], and Bruce M. McGEOCH[3]
[1]Thermal Energy System Specialists, LLC – Madison, WI (USA)
[2]Thermal Storage Solutions, LLC – North Ryegate, VT (USA)
[3]BlueJag Consulting, LLC – South Burlington, VT (USA)

ABSTRACT

This paper presents the simulation model of a residential scale solar heated seasonal thermal storage system constructed in central Vermont. Performance data was recorded at the site between January and April 2009 and an exercise was carried out to estimate appropriate parameters for the modeled heat exchanger, solar collector, and seasonal storage bed based on measured data. With the exception of the load-side heat exchanger outlet temperature, calibrated model results matched simulation extremely well and provided confidence in the previously unvetted storage bed model. Both data and simulation suggest that the bed's effective storage capacity is significantly lower than its size would suggest. Longer term data monitoring is necessary in order to reach a conclusion on this question.

INTRODUCTION

Solar thermal seasonal storage systems intended to meet the space heating needs of individual residences have been proposed and assessed in a number of previous studies (eg. Hugo, 2007). For the most part, these studies have come to the conclusion that such systems are technically feasible. Experience among the authors, however, has been that unless climatic conditions are ideal, such systems become cost prohibitive before they significantly impact purchased energy costs. Actual proposed and constructed systems tend to be district based, spreading the cost over many residences (Chapuis, 2009) and (Sibbitt, 2007). However, many of the previously proposed systems rely on comparatively expensive vertical bore holes and ground energy storage. In early 2008, a less expensive ground storage alternative was proposed, and through a TRNSYS (Klein, 2005) simulation was shown to have enough potential that a pilot project was constructed and outfitted with temperature and flow-rate monitoring equipment late that year. In this case, the storage consists of an excavated volume of earth, highly insulated on its outer walls, backfilled with wet sand, capped with significant insulation and then top-filled to grade-level with soil. Energy is added to the storage media by flowing solar-heated water through a punctured pipe network buried near the top of the storage bed (similar to a drip irrigation system). Water filters through the bed (nominally of its own accord) and is recuperated from a sump at the bottom from which it is filtered and returned to the solar collectors. The load side of the storage system consists of a heat exchanger buried about one third the depth of the storage bed; water flows into and out of the load heat exchanger by means of a pump that connects it to the residence's existing space heating system.

While it would have been advantageous from an energy standpoint to use an entirely water-based thermal storage (the specific heat of water being four times that of sand) the storage vessel for an appropriate quantity of water was quite a lot more expensive than the proposed wetted media storage. Furthermore, buried water-filled storage posed structural concerns not encountered by the sand-filled storage.

Figure 1 shows a schematic representation of the system. The figure indicates the major system components, the locations of the temperature sensors (T-Sxx) and the locations of the flow rate sensors (M-Fxx).

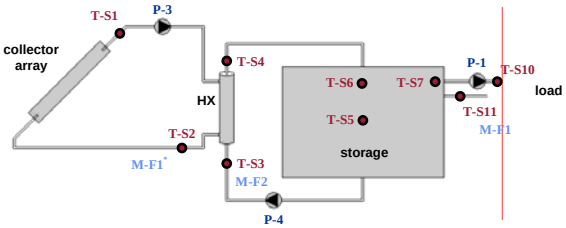

Figure 1: System Schematic

HEAT EXCHANGER PARAMETER ESTIMATION

The heat exchanger appeared to be the simplest place to start the parameter estimation exercise; inlet and outlet temperatures were recorded on either side of the shell and tube device and the thermal properties of the load-side fluid (water) were known with a good degree

of confidence. Temperatures were measured by means of thermocouples placed at the inlets and outlets; temperature differences were calculated from the readings. While the flow rate on the storage side was also recorded, the flow rate on the collector side was known only based on pump ratings and on spot measurements performed using an installed sight glass. The thermal properties of the water/glycol mixture on the collector side of the heat exchanger were calculated based on a volumetric ratio of component properties and were therefore not as well known as the properties of the water on the load side. The properties of the water/glycol mixture were assumed to be constant over the operating temperature range of the system. This is probably a source of error in the calibrations since experience with the system showed that at colder temperatures, the mixture was quite sludgy. In order to minimize the impact of the constant properties assumption, parameter estimation was performed based only during times when the system had been running for at least 10 minutes.

Prior to parameter estimation, the heat exchanger data was examined to find periods of clean recorded information (free from data collection gaps). The early identified periods lasted one to two weeks in February but showed an average 30% energy imbalance based on calculating $m*Cp*\Delta T$ for each side of the heat exchanger. A faulty check-valve was found on the load side of the heat exchanger piping and reduced the average energy imbalance to 15%. No other faults in the system or data collection could be identified and attention turned to the mass flow rate on the collector side, which had been estimated using a spot measurement through a sight glass in the piping. The mass flow rate was instead back-calculated (forcing energy to balance across the heat exchanger) for all times when the pumps had been operating for at least ten minutes. The average of the calculated mass flow rates was 0.145 L/s, approximately 10% higher than had been originally estimated and well within the measurement uncertainty. Recalculating using the newly estimated collector side flow rate resulted in an average 10% energy imbalance over a 20 day period of clean data in March.

There are a number of possible reasons for the remaining energy imbalance across the heat exchanger. First, the flow rate on both sides of the heat exchanger was assumed to be steady over each 10 minute time step when in fact the recorded data represented an average over the same period. Second, as previously mentioned, the thermal properties of the glycol/water mixture on the collector side was assumed to be constant over the heat exchanger operating range. Third, jacket thermal losses form the heat exchanger were neglected. In fact the heat exchanger is uninsulated, and was installed in a constructed box containing a heater to keep it from freezing; the gains from that heater could well have affected the energy balance but environment temperature near the exchanger was not monitored or recorded. Lastly, and again because environment temperature was not monitored, line losses between the collector outlet and the heat exchanger inlet were neglected and in fact, the "heat exchanger inlet temperature" was measured at the collector outlet as indicated in Figure 1.

In order to estimate parameters for the heat exchanger model, a simulation was developed consisting of the heat exchanger alone (using a simple constant effectiveness model) driven with measured temperature at both inlets and measured flow on the storage side. The optimization variables were the flow rate on the collector side and the heat exchanger effectiveness. The optimization tool (GenOpt) (Wetter, 2009) sought to minimize the difference between the measured and simulated outlet temperatures on both sides of the heat exchanger but only when there was flow on both sides of the exchanger for at least ten minutes. The optimization algorithm found the best-fit heat exchanger effectiveness to be 0.54 (10% lower than the originally estimated 0.60) and found the collector flow rate to be unchanged from the originally assumed 0.145 L/s. Figure 2 shows the measured and (calibrated) simulation outlet temperature for the source (2a) and load (2b) sides.

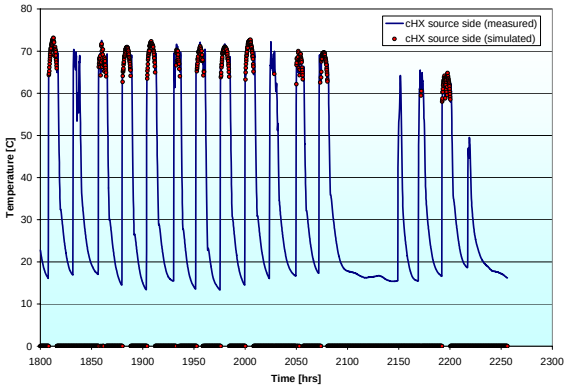

Figure 2a: Measured and Simulated Collector-Side Outlet Temperature

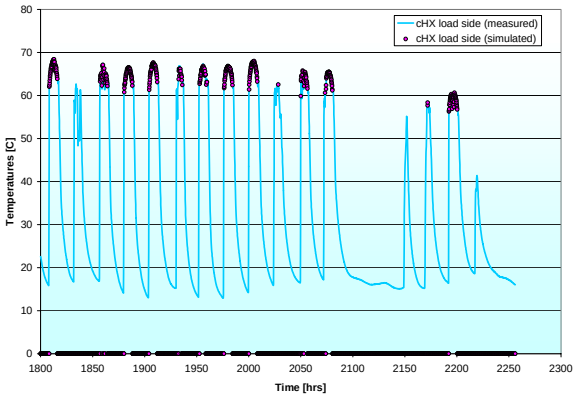

Figure 2b: Measured and Simulated Storage-Side Outlet Temperature

SOLAR COLLECTOR PARAMETER ESTIMATION

The solar collector parameter estimation was perhaps the most straightforward of the three. The collectors were evacuated tube Beijing Sunda Seido5 panels. Initial estimates of the collector performance parameters were taken from the SRCC OG-100 certification sheets for the panels. In addition to temperature and flow rate into the collectors, the total solar radiation on the plane of the array had also been recorded. The collector model, however, treats the different components of solar radiation (beam, sky diffuse, and ground reflected diffuse) separately. The HDKR (Duffie, 1991) model was used to determine the best split between beam and diffuse. Temperatures were again measured by thermocouple and temperature differences were calculated. As with the heat exchanger parameter estimation, the optimization algorithm minimized the difference between measured and simulated collector outlet temperature only when the collector pump had been on for at least 10 minutes. The originally estimated collector parameters are shown in

Table 1; the optimization variables (collector thermal capacitance, intercept efficiency, and 1st order efficiency coefficient) are shown in bold.

Table 1: Collector Parameters from SRCC OG-100 Rating

Collector area	16.338	[m²]
Fluid specific heat	3.1188	[kJ/kg.K]
Tested flow rate per unit area	36	[kg/h.m²]
Fluid specific heat at test conditions	4.190	[kJ/kg.K]
1st order IAM coefficient	-0.9474	[-]
2nd order IAM coefficient	1.0762	[-]
Collector thermal capacitance	***160***	***[kJ/K]***
Intercept efficiency (a0)	**0.48**	**[0..1]**
1st order efficiency coefficient (a1)	**5.7078**	**[kJ/h.m².K]**
2nd order efficiency coefficient (a2)	0.08172	[kJ/h.m².K²]

Figure 3 shows the calibrated collector model simulation outlet temperature as well as the measured outlet temperature.

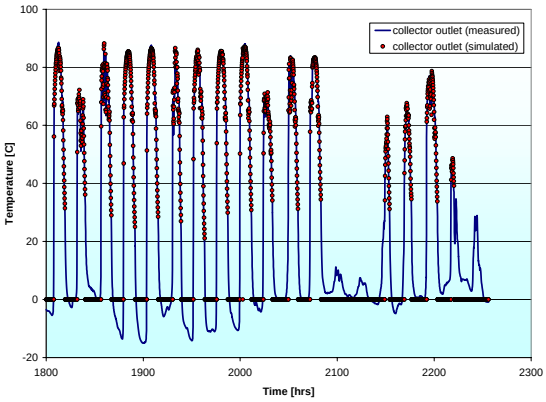

Figure 3: Measured and Simulated Collector Outlet Temperature

The optimized intercept efficiency was 0.459 (4% lower) and the optimized loss coefficient was 6.2 kJ/h.m².K (9% higher). The optimized collector capacitance was 4 kJ/K, which is suspiciously low. The collector thermal capacitance's primary effect is on how quickly the collector heats up and cools down. In many models, this effect is ignored and the low value resulting from the optimization would indicate that the thermal capacitance of the array itself could be ignored here too. However, it is suspected that because the error function for optimization was only evaluated once

the collector had been running for at least 10 minutes, that the transient behaviour of the collector was already being ignored and thus the capacitance didn't come into play. It is recommended that the collector be re-optimized using some summer data when freezing (and the consequent changes in the viscosity of the water/glycol mixture in the collector loop) would not be a problem and would allow optimization during start and stop cycles as well as during fully developed flow.

THE STORAGE MEDIA MODEL

The storage bed consists of a somewhat irregularly shaped excavated pit whose walls are heavily insulated with a liner and a high density spray-on foam and which is then backfilled with sand and capped. The bottom of the pit is sloped to a sump. A layer of piping embedded in the media near the top of the backfilled pit flows solar heated water into the media. Energy is removed from (or could be added to) the media bed by means of two layers of piping, one layer located 1/3 of the way up from the bottom and a second layer of piping located 1/3 of the way down from the top.

The model used to predict the behaviour of the thermal storage bed was one that had originally been developed to model the thermal behaviour of wetland cells (TESS, 2004). A wetland cell in this case is essentially a rectangular parallelepiped that may be partially buried in the ground. In the present case, the cell is entirely buried. The cell is assumed to be filled with some kind of porous media such as gravel and can be capped by a transparent or an opaque cover (opaque in this case). Air and liquid may be pumped into and/or removed from the cell. When liquid is pumped in or drawn out, a corresponding amount of air is entrained into or pushed out of the cell. The model assesses the energy transfers between the liquid, the media, the cell itself, the surrounding ground, and the ambient.

The storage bed is modeled much like a liquid filled thermal storage tank with a number of horizontally-oriented, equal volume nodes each representing the temperature of a layer within the bed. The model assumes that within a given node, the media is at a uniform temperature, and that the liquid and air are fully mixed at uniform temperatures. The media, air, and liquid temperatures within a node may, of course, be different and if the cell is allowed to sit idle, those temperatures will come to an equilibrium.

This model differs from other thermal storage tank models in that the volume of liquid contained within the bed may change with time. The bed is assumed to be completely filled with a homogenous porous media (such as gravel) and depending upon the rate at which liquid is being added to and / or removed from the cell, the interstitial spaces within the media are filled either by liquid or by air. In this particular application, any water removed from the bottom of the bed is returned to the top so the water level stays at its starting level (approximately 2/3 full). In reality, the bed is filled with a more porous media near the bottom (gravel) and a less porous media above (sand). The two levels are separated by a perforated cloth to prevent sand from getting into the sump. It was decided early in the project to try and estimate parameters for the model before going to the trouble of allowing for non-homogenous media void fractions within the bed.

Another departure from most thermal storage tank models is that the storage bed is fully or partially buried in the ground. As such, energy transfer between the cell and ambient and between the cell and the surrounding ground are both calculated. In order to calculate conduction between the cell and the surrounding soil, a volume of soil (called the near-field) is defined. The near-field extends away from the edges of the rectangular wetland cell in three dimensions as shown in Figure 4.

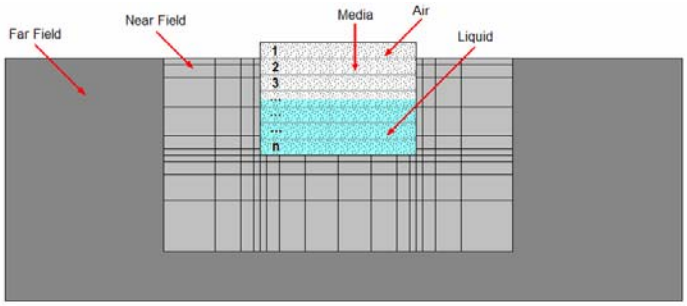

Figure 4: Section View of the Storage Bed, Near, and Far-Fields

The storage bed model solves five coupled nodal differential equations at each iteration and at each time step of the simulation. The five differential equations are a near-field soil energy balance, a liquid node energy balance, a sensible air node energy balance, a latent air node energy balance, and a media energy balance. Equations are written for fully filled air and fully filled liquid nodes as well as for the node that contains the air/liquid boundary. The node containing the air/liquid boundary is referred to as the liquid level node. Solving these coupled equations becomes more difficult when the mass of liquid and air are changing within a given node. The solution becomes more difficult still if a node completely fills or completely empties during a simulation time step. When the user specifies an inlet or outlet liquid flow rate the model checks to see whether the liquid level node will

completely fill or completely empty before the end of the time step. If it will, then the model determines the amount of time before the node fills or empties and solves the differential equations based on that reduced time step. It then calculates the time that remains in the time step and solves the differential equations for the fully empty or fully filled node. It is necessary to break the time step into sub time steps and solve the coupled differential equations twice for such a time step: once for the portion of the time step when node n is partially liquid and partially air filled and once for the second part of the time step when node n-1 is the liquid level node. If a case occurs in which more than two nodes are the liquid level node at one point in the time step then it is necessary to break the time step up into sufficient parts.

One other simplification that the model makes is that it becomes very difficult to solve the coupled differential equations when the mass of liquid or the mass of air in a node goes to zero. Therefore a very small mass of air is assumed to remain in a node when that node is completely filled with liquid. The temperature of the air is assumed to be at the temperature of the media node and at 100% relative humidity. Likewise, a very small mass of liquid is assumed to remain in a node when the node is completely emptied of liquid. The temperature of the fluid is assumed to be at the temperature of the media node.

A number of the model's simplifying assumptions are non-ideal for the present storage bed application:

First, the model assumes that the media is porous enough that liquid entering a node above the liquid level node does not spend enough time filtering down to the liquid level node to impact the media temperature in the nodes through which it passes. In the present case, the bed is filled with sand, which has a low porosity; the water is intended to filter slowly down through the bed, giving up most of its energy near the top and promoting thermal stratification.

Second, the model assumes that the storage bed is a rectangular parallelepiped and while this is generally true, the actual studied bed does not have a uniform depth.

Third, the model assumes that the storage bed temperature is uniform and allows thermal stratification to develop over time. Fortunately, the measured data indicated that the bed was at a fairly uniform temperature at the start of the calibration period.

Fourth, the model does not account for horizontal temperature variation within the bed. It is difficult to know how much of an impact this assumption had as there was only one temperature sensor near the edge of the storage bed and it was positioned close enough to the heat exchanger outlet that its recorded temperature was more dominated by the temperature of the heat exchanger than it was by the dynamics of the bed itself.

PARAMETER ESTIMATION OF THE STORAGE MEDIA

The 1.8m deep by 6m long by 4.5m wide was outfitted with three temperature sensors; one in the middle both vertically and horizontally (T-S5), one in the middle horizontally but near the top vertically (T-S6) and one at the same vertical placement as T-S6 the but near the edge (T-S7) at which the load-side heat exchanger enters and exits. Budget limitations prohibited a more comprehensive mapping of temperatures in the bed.

The storage bed parameters from the original simulation bed were estimated as shown in Table 2.

Table 2: Storage Bed Model Parameters (prior to parameter estimation)

Storage height	1.829	[m]
Storage length	5.988	[m]
Storage width	4.562	[m]
Depth of storage bottom	2.1338	[m]
Storage wall loss coefficient	0.024418	[kJ/h.m^2.K]
Storage tank divisions	4	[-]
Media specific heat	***0.83***	***[kJ/kg.K]***
Media density	1602	[kg/m^3]
Media thermal conductivity	***1.26***	***[kJ/h.m.K]***
Media void fraction	0.05	[0..1]
Total media surface area	10000	[m^2]
Initial storage temperature	60.68	[C]
Initial fill fraction	1	[0..1]
Fluid specific heat	4.19	[kJ/kg.K]
Fluid density	1000	[kg/h]

Fluid thermal conductivity	2.204	[kJ/h.m.K]
Fluid kinematic viscosity	3.2	[kg/m.h]
Soil conductivity	4.68	[kJ/h.m.K]
Soil density	2100	[kg/m^3]
Soil specific heat	0.96	[kJ/kg.K]
Mean surface temperature	7.21	[C]
Amplitude of surface temperature	12.53	[deltaC]
Day of minimum surface temperature	37	[day]
Heat exchanger location	2	[-]
Heat exchanger effectiveness	***0.3***	***[0..1]***
Specific heat of heat exchanger fluid	4.19	[kJ/kg.K]

The parameters shown in bold (media specific heat, media thermal conductivity, and load-side heat exchanger effectiveness) were those selected as parameter estimation variables. While there were certainly other parameters whose values were very hard to guess (void fraction and total media surface area for

example), care had to be taken not to let the optimization algorithm have too many variables to tune. Calibrations were again performed using GenOpt. This time, the optimization sought to minimize the sum of the differences between

- the T-S5 measurement and the simulated temperature of the middle node of the bed
- the average of the T-S6 and T-S7 measurements and the simulated temperature of the top node of the bed.
- the T-S3 measurement and the simulated outlet temperature of water leaving the sump when there is source flow.
- the T-S10 measurement and the simulated outlet temperature of water leaving the load side heat exchanger when there is load flow.

The result of the calibrations are shown below. Figure 5 shows the measured and simulated temperatures in the middle of the bed.

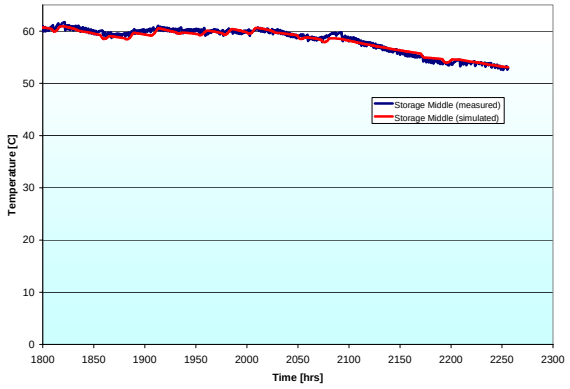

Figure 5: Measured (blue) and Simulated (red) Temperature at the Middle of the Storage Bed (T-S5 location)

Figure 6 shows the measured and simulated temperatures in the middle of the bed. The measured temperature in this case is the average of the T-S6 (top middle) and the T-S7 (top side) locations. It was decided to use the average of these two temperatures because the storage bed model does not allow for horizontal temperature variation; the bed is allowed to stratify only along the vertical axis.

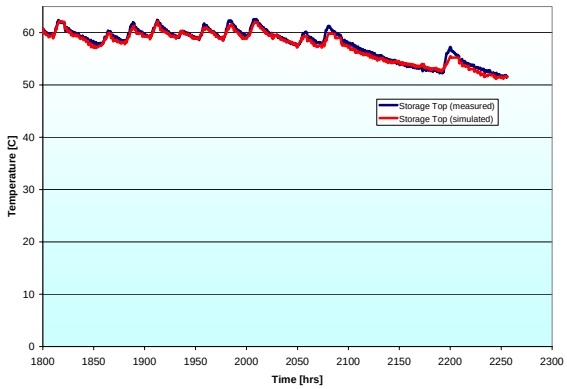

Figure 6: Average Measured (blue) and Simulated (red) Temperature at the Top of the Storage Bed (T-S6 and T-S7 locations)

Figure 7 shows the measured and simulated temperature at the outlet of the load-side heat exchanger. It seems apparent from the data and the figure that there is something wrong with the load side heat exchanger temperature measurement. The data shows spikes in outlet temperature following shortly on the heels of the pump turning off and there is not good correlation between the simulation and the measurements even when liquid has been flowing through the heat exchanger for some time. Given that the measured and simulated temperatures of the media just inside the bed near the load side heat exchanger outlet correlate well (Figure 6) and that the measured load-side heat exchanger outlet temperature bears very little resemblance to the of the temperature profile just inside the bed, it is suspected that the measurement of the heat exchanger outlet temperature was faulty due to an incorrect placement of pumps and check-valves at the load-side heat exchanger inlet and outlet ports. The connections have been corrected but post-correction data is unfortunately, unavailable.

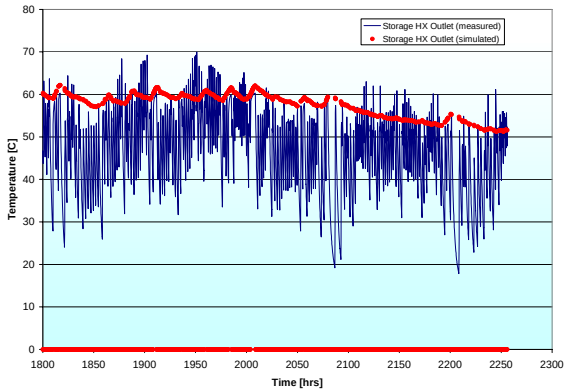

Figure 7: Measured (blue) and Simulated (red) Load-Side Heat Exchanger Outlet Temperature (T-S10 location)

Figure 8 shows the measured and simulated temperature of liquid exiting the bottom of the storage and returning to the source-side heat exchanger (and thereby the collector loop). Points are plotted only when there is flow on the source side of the bed.

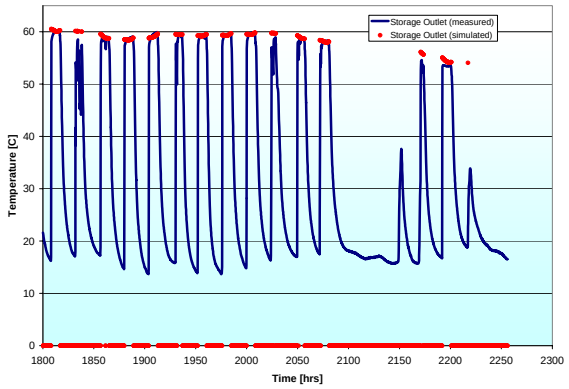

Figure 8: Measured (blue) and Simulated (red) Storage Bed Outlet Temperature (T-S3 location)

Calibration resulted in a heat exchanger effectiveness of 0.363 (21% higher than initially guessed), a media specific heat of 0.53 kJ/kg.K (35% lower than initially guessed), and a media thermal conductivity of 19 kJ/h.m.K, which was deemed to be unrealistically high. The initial guesses of media thermal properties came from published property data for dry sand (the water is handled separately from the media in the model so it is not appropriate to use property data for wet sand). It is surprising that there would have been such significant difference in thermal properties of the media in the storage bed and the published values. It is much more likely that there is some other behaviour in the system not currently accounted for in the model which has the effect of dramatically raising the effective thermal conductivity and decreasing the effective specific heat. Or, in simpler terms, makes the thermal storage bed react to driving forces as though it were much smaller than it actually is.

One possibility is that there is a great deal more energy exchange between the media and the water than is modeled by the "total media surface area" and the "convection coefficient between media and water" parameters. Indeed rerunning the parameter estimation and allowing these two variables to be optimized instead of the media thermal properties resulted in a higher surface area and a higher convection coefficient.

Another possibility for the lower than expected bed capacity is the pipe network that flows source water into the media at the top of the storage. Very little is known about the flow pattern in this network; the network is intended to spread the inlet source flow evenly across the top of the media in the bed but it may be that most of the source water is being emptied into a small area and is flowing in a comparatively narrow column down to the sump, thereby causing the effective storage capacity of the bed to appear lower than its actual size would suggest.

CONCLUSIONS

It is felt that the parameter estimation of the solar collector and heat exchangers are accurate given the data that has been presented. While the parameter estimation of the storage bed showed good correlation between measured and simulated results and raised the confidence level in a previously unvetted model, it also raised a number of questions that bear further study. Based on the data collected during the first part of the year, the storage bed acts as though it is smaller than its actual size (i.e. it changes temperatures faster than would have been expected). Longer term data monitoring and a more extensive network of temperature sensors deployed in the bed would go a long way toward explaining the underlying causes. Unfortunately, lighting during a spring storm added an unwanted dose of reality to the parameter estimation exercise and the system is only now starting to record data again. A second pilot system is in the design phase at this time and will allow for the installation of more temperature sensors in the storage bed.

Another possibility for the lower than expected capacity is volatility of the sample period. During the analysis period, the load (house) was in high demand for energy from the storage, which may mean that the collected energy deposited in the storage was quickly removed on an hourly basis before the heat transfer fluid (water) could affect the entire volume of storage media. The effect on the data would be consistent with the analysis and longer term data analysis, coupled with a more comprehensive grid of temperature sensors placed vertically and horizontally in the media would be desirable.

REFERENCES

Hugo, A., R. Zmeureanu, and H. Rivard "Modeling of a Seasonal Thermal Storage System in a Residential Building" http://www.solarbuildings.ca/c/sbn/file_db/Modelling%20of%20a%20seasonal%20thermal%20storage%20system.pdf

Chapuis, S., and M. Bernier, (2009) "Seasonal Storage Of Solar Energy In Borehole Heat Exchangers." SimBuild09 : Proceedings of the International Building

Performance Simulation Association World Conference.

Sibbitt, B., T. Onno, D. McClenahan, J. Thornton, A. Brunger, J. Kokko, B. Wong. (2007). “The Drake Landing Solar Community Project – Early Results,” 2nd Canadian Solar Buildings Conference, Calgary (Alberta), Canada.

Klein, S.A. et al. (2005), TRNSYS: A Transient Simulation Program. Madison, WI: Solar Energy Laboratory, University of Wisconsin – Madison

Wetter, M. et al. (2009), GenOpt: Generic Optimization Program. Berkeley, CA: Lawrence Berkeley National Labs.

Duffie, J.A. and W.A. Beckman, Solar Engineering of Thermal Processes. 2nd edition, New York: John Wiley and Sons, Inc., 1991

TESS (2004), “TESS Libraries v. 2, User Manual” Thermal Energy System Specialists, LLC, Madison, WI, USA.